PCCP

ROYAL SOCIETY OF CHEMISTRY

PAPER

Cite this: *Phys. Chem. Chem. Phys.*, 2020, **22**, 5123

Interaction of positronium with dissolved oxygen in liquids†‡

P. S. Stepanov, *[a] F. A. Selim, [a] S. V. Stepanov, [bc] A. V. Bokov, [b] O. V. Ilyukhina,[b] G. Duplâtre[d] and V. M. Byakov [be]

Received 11th November 2019,
Accepted 29th January 2020

DOI: 10.1039/c9cp06105c

rsc.li/pccp

The interaction of positronium (Ps) with molecular oxygen dissolved in liquids is experimentally investigated. Computer software has been developed for fitting the positron annihilation lifetime spectra in liquids using parameters with clear physical meaning: rate constants of the Ps chemical reactions, annihilation rate constants of the different positron states, probability of Ps formation in a quasi-free state, typical formation time of a Ps nanobubble. Such processing of the spectra allowed identification of the dominant interaction of the Ps atom with dissolved oxygen. It turns out to be mainly *ortho–para*-conversion (Ps → 1/4 *p*-Ps + 3/4 *o*-Ps), but not oxidation (Ps + O_2 → e^+ + O_2^-). Values of the reaction rate constants are obtained.

1. Introduction

Positron annihilation spectroscopy (PAS) has numerous applications in materials science such as in studies of structural defects, free volume and porosity of materials. At the same time PAS is also applied to study radiolytic processes in chemistry, radiobiology and medicine.[1]

In experiments with radioisotope positron sources, positrons are born and injected into the studied material with a continuous energy distribution, with the end point energies 1.47 MeV for a ^{44}Ti–^{44}Sc–^{44}Ca-source and 0.54 MeV for a ^{22}Na–^{22}Ne-source. During ionization the slowing down positrons form tracks (clusters of ion–electron pairs along their trajectory), and after becoming thermalized e^+ start to explore the surrounding medium. Because typical lifetimes of the positron states (0.1–10 ns) are of the order of characteristic times of intratrack processes in molecular media, the positron turns out to be a convenient probe for radiation phenomena.

In nonconducting (molecular) substances, a thermalized e^+ easily forms Ps, which is a bound state of e^+ and e^- (the lightest analog of a hydrogen atom). The formation of Ps occurs in the final part of the e^+ track (the positron blob) as a result of the combination of a thermalized positron with one of the track electrons. Depending on the relative orientation of e^+ and e^- spins, the Ps atom can exist either in the *para*-state (*p*-Ps), with a spin equal to zero, or in the *ortho*-state (*o*-Ps), with a spin equal to $1{\cdot}\hbar$.[2]

In most molecular liquids, the *o*-Ps lifetime is much shorter than *in vacuo* (142 ns). It is decreased to a few ns because of the so-called pick-off process, when the positron (in Ps) undergoes 2γ-annihilation with one of the nearest molecular electrons, whose spin is anti-parallel to the positron spin. Nevertheless, the *o*-Ps atom can take part in chemical reactions not only with intratrack radiolytic products (in water, these are hydrated electrons, H_3O^+, OH-radicals), but also with dissolved substances, for example molecular oxygen, O_2.[3]

Recently, some interest in the phenomenon of shortening of the *o*-Ps lifetime (Ps quenching) in various liquids due to its interaction with dissolved oxygen has reemerged. This effect seems to be important when testing healthy and carcinogenic tissues by means of PAS because the oxygen content therein noticeably differs.[4] The reason is the so-called oxygen effect: there are relatively few blood vessels in cancerous tumors, so cancer cells develop under oxygen-poor conditions. This explains the enhanced radioresistance of the cancer cells, since only the products of the interaction of dissolved oxygen with the chemically active radicals (which appear because of irradiation) destroy the tumor. PAS studies in this direction are partially stimulated because of the development of a new type of positron annihilation tomographer at the Jagiellonian University in Krakow, Poland.[5,6]

[a] *Center for Photochemical Sciences, Department of Physics and Astronomy, Bowling Green State University, OH 43403, USA. E-mail: petrs@bgsu.edu, faselim@bgsu.edu*

[b] *Institute for Theoretical and Experimental Physics named by A.I. Alikhanov of National Research Centre "Kurchatov Institute", Moscow, 117218, Russia. E-mail: stepanov@itep.ru, av.bokov@yandex.ru, ilyukhina@itep.ru, byakov@itep.ru*

[c] *National Research Nuclear University "MEPhI" (Moscow Engineering Physics Institute), Moscow, 115409, Russia*

[d] *Institut Pluridisciplinaire Hubert Curien, CNRS/IN2P3, BP 28 67037 Strasbourg, Cedex 2, France. E-mail: gduplatre@estvideo.fr*

[e] *D. Mendeleyev University of Chemical Technology of Russia, Miusskaya sq., 9, Moscow, 125047, Russia*

† PACS/topics: 78.70.Bj, 82.30.Gg, 36.10.Dr.

‡ Electronic supplementary information (ESI) available. See DOI: 10.1039/c9cp06105c

The interaction of Ps with oxygen molecules (as well as with some molecules possessing oxidizing properties, such as Cl_2, Br_2, I_2) is more important than with other neutral molecules (for example, N_2). The interaction with neutral molecules through elastic collisions leads to the pick-off annihilation of Ps; the time of such a collision is very short. By contrast, Ps interaction with oxygen molecules results in the formation of an activated unstable complex or compound (PsO_2 or $e^+O_2^-$); the time involved can thus be much longer. The O_2 molecule can either oxidize the Ps atom ($Ps + O_2 \rightarrow e^+ + O_2^-$) or stimulate its *ortho–para* conversion ($Ps \rightarrow 1/4\ p\text{-Ps} + 3/4\ o\text{-Ps}$), because the O_2 molecule has a magnetic moment. All these processes lead to an observable decrease of the *o*-Ps lifetime (Ps quenching).[7–11] Using conventional methods of processing of the positron annihilation lifetime (LT) spectra it is impossible to distinguish between oxidation and spin-conversion reactions.

Experiments with magnetic fields indicated the importance of the Ps *ortho–para* conversion and allowed the estimation of the decrease of the Ps contact density parameter ($\eta_c = |\Psi^{Ps}_{liquid}(0)|^2/|\Psi^{Ps}_{vacuum}(0)|^2$) in only a few liquids: water (0.8; 0.65), benzene (0.84), methanol (0.68) and hexane (0.82).[12,13] So we assume that η_c is about 0.75–0.8 in all liquids studied here. It means that *para*-Ps, being in a bubble state in a liquid, lives about 160 ps (longer than under vacuum) before it undergoes 2γ-annihilation.

In this paper, we present the results of our PAS experiments in organic liquids (cyclohexane, isooctane, isopropanol) and in water in order to identify the nature of the Ps–O_2 interaction (oxidation or conversion). Values of the reaction rate constants are obtained with the help of new software, which uses an advanced model of Ps formation for processing LT annihilation spectra.

2. Experimental

All the reagents used were purchased from Russian Chemist (www.rushim.ru). Unlike previous studies,[8,9] we did not use the freeze–thaw method to remove dissolved O_2 to avoid the risk of damaging the positron source during freezing and evacuation. Therefore, oxygen was removed from the liquid phase by bubbling with chemically pure argon. For determination of the rate constants of the Ps + O_2 reactions, the liquids were bubbled either with air or pure oxygen to increase the O_2 concentration.

The gases were previously cleaned by means of blowing them through dry alkali KOH and then through Metrohm 0.3 nm nanosieves previously kept for 24 h under vacuum at 250 °C. Next, the purified gas was fed into a hermetically sealed vial containing the studied liquid. Input/output of the gas was performed by means of two long medical needles tightly inserted into the lid of the vial.

The positron source was made from a 10 mm diameter, 0.2 mm thick titanium washer. Its central part (6 mm diameter) was welded on both sides with 10 μm titanium foils. In between them a radioactive powder of $TiCl_4$, containing about 7.5 MBq of ^{44}Ti, was deposited. The positron source was fixed in the center of the vial using a stainless steel clip. The clip itself was tightly fixed in the lid of the vial. The source correction was determined by a series of separate measurements of the reference (pure, well-annealed) samples (Al, Si, Fe and W). From these measurements we concluded that for the present experiments with liquids the source correction is 13%. It consists of the following components: I_1 = 32%, t_1 = 0.15 ns; I_2 = 50%, t_2 = 0.38 ns; I_3 = 18% and t_3 = 1.8 ns.

The lifetime annihilation spectra were recorded using two γ-detectors with BaF_2 scintillators and fast timing nanosecond electronic units from ORTEC. The time resolution of the annihilation spectrometer was 280 ps. Spectra were recorded sequentially for each hour during one day. The total number of "start-stop" coincidences in each spectrum was about 1 million. All measurements were done at 20 °C.

The spectra were first analyzed through 3-exponential deconvolution. The lifetime of the shortest (parapositronium) component was fixed to the lifetime of *p*-Ps in a vacuum, 125 ps. Then, a more accurate model was used, taking into account the formation of a quasi-free positronium and its subsequent transformation into a bubble state.

3. *Ortho–para* conversion and oxidation of Ps in the presence of dissolved O_2

Immediately after its birth, as a result of the radioactive transformations of ^{44}Ti–^{44}Sc–^{44}Ca radioactive nuclei, the positron has a rather large kinetic energy (about 1 MeV). Within the next 10 ps, it loses its energy to thermal energy because of ionization slowing down. At the end of its track in molecular media, the thermalized positron can combine with one of the electrons knocked out through ionization along the track. This process results in the formation of quasi-free positronium, qf-Ps, a delocalized weakly bound state of e^+ and e^-, which also moves in a liquid at thermal velocity.[14,15] Note that there is no need to specify the spin state of qf-Ps, because the contact density of its electron at the level of the positron is rather small. Therefore, the main channel of qf-Ps annihilation is annihilation of e^+ with one of the electrons of the surrounding molecules. Within 50–100 ps, qf-Ps transforms into a localized state (Ps bubble formation time).[16,17] Although the typical qf-Ps lifetime is rather short, this state is important for explaining the extreme behavior of the *S*-parameter time dependence in AMOC experiments.

In the following scheme, we neglect initial picosecond-scale processes like electron and positron solvation, and qf-Ps formation. The initial moment (t = 0) of the following system describing transformation of the positron states is the time moment of formation of qf-Ps:

$$\dot{n}_+(t) = -\lambda_+ n_+ + \lambda_{ox} n_o, \quad n_+(0) = 1 - P_{qf}, \tag{1}$$

$$\dot{n}_{qf}(t) = -\lambda_q n_{qf}, \quad n_{qf}(0) = P_{qf}, \quad \lambda_q = \lambda_{qf} + \lambda_b, \tag{2}$$

$$\dot{n}_o(t) = \frac{3\lambda_b}{4} n_{qf} - \lambda_o n_o, \quad n_o(0) = 0, \qquad \lambda_o = \lambda_{po} + \frac{\lambda_{opc}}{4} + \lambda_{ox}, \tag{3}$$

$$\dot{n}_p(t) = \frac{\lambda_b}{4} n_{qf} + \frac{\lambda_{opc}}{4} n_o - \lambda_p n_p, \quad n_p(0) = 0, \qquad \lambda_p = \lambda_{2\gamma} + \lambda_{po}. \tag{4}$$

Here, $n_+(t)$ and $n_{qf}(t)$ are the probabilities of the existence of the thermalized solvated positron and qf-Ps at time t, respectively; $n_o(t)$ and $n_p(t)$ are the probabilities of observing the Ps atom localized in a bubble in the *ortho*- and *para*-state, respectively; $\lambda_b = 1/(0.05\text{–}0.1\ \text{ns})$ is the rate constant of the qf-Ps transformation into positronium localized in a nanobubble; P_{qf} is the formation probability of qf-Ps; λ_{qf} and λ_+ are the annihilation rate constants of the qf-Ps and solvated positron; λ_{po} is the pick-off annihilation rate constant of Ps; and $\lambda_{ox} = k_{ox} c_{O_2}^{(L)}$ and $\lambda_{opc} = k_{opc} c_{O_2}^{(L)}$ are the oxidation and *ortho–para* conversion rate constants. $c_{O_2}^{(L)}$ is the concentration of molecular oxygen and $\lambda_{2\gamma} \approx 8\ \text{ns}^{-1}$ is the 2γ annihilation of *p*-Ps. In the above equations we neglected the *para*-to-*ortho* process since, due to the rather low O_2 concentrations used, this reaction appears kinetically negligible compared to the fast 2γ-decay of *p*-Ps. Solving eqn (1)–(4) gives the following equations for all 4 positron states:

$$n_{qf}(t) = P_{qf} e^{-\lambda_q t}, \quad n_o(t) = \nu\left(e^{-\lambda_o t} - e^{-\lambda_q t}\right), \quad \nu = \frac{3P_{qf}}{4}\frac{\lambda_b}{\lambda_q - \lambda_o}, \tag{5}$$

$$n_+(t) = (1 - P_{qf}) e^{-\lambda_+ t} + \nu\frac{\lambda_{ox}}{\lambda_+ - \lambda_o}\left(e^{-\lambda_o t} - e^{-\lambda_+ t}\right) - \nu\frac{\lambda_{ox}}{\lambda_q - \lambda_+}\left(e^{-\lambda_+ t} - e^{-\lambda_q t}\right), \tag{6}$$

$$n_p(t) = \frac{P_{qf}}{4}\frac{\lambda_b}{\lambda_q - \lambda_p}\left(e^{-\lambda_p t} - e^{-\lambda_q t}\right) + \nu\frac{\lambda_{opc}/4}{\lambda_p - \lambda_o}\left(e^{-\lambda_o t} - e^{-\lambda_p t}\right) - \nu\frac{\lambda_{opc}/4}{\lambda_q - \lambda_p}\left(e^{-\lambda_p t} - e^{-\lambda_q t}\right). \tag{7}$$

2γ-Annihilation of these four positron states gives the following contribution to the shape of the LT spectrum:

$$C_{2\gamma}(t) \propto \lambda_{qf} n_{qf} + \lambda_+ n_+ + \lambda_p n_p + \lambda_{po} n_o. \tag{8}$$

Thus, in this case the LT spectrum consists of 4 exponentials:

$$C_{2\gamma}(t) \propto \lambda_q I_0 e^{-\lambda_q t} + \lambda_p I_1 e^{-\lambda_p t} + \lambda_+ I_2 e^{-\lambda_+ t} + \lambda_o I_3 e^{-\lambda_o t}. \tag{9}$$

Of course, to compare this with the experiment, we must add the contribution from e^+ annihilation within the positron source, convolute $C_{2\gamma}(t)$ with the resolution function of the spectrometer, and add a random coincidence background. Combining the terms corresponding to the same exponents, we find the intensities:

$$\begin{aligned} I_0 &= P_{qf}\frac{\lambda_{qf}}{\lambda_q} - \frac{P_{qf}}{4}\frac{\lambda_p \lambda_b}{\lambda_q(\lambda_q - \lambda_p)} + \nu\frac{\lambda_p \lambda_{opc}/4}{\lambda_q(\lambda_q - \lambda_p)} \\ &\quad + \nu\frac{\lambda_+ \lambda_{ox}}{\lambda_q(\lambda_q - \lambda_+)} - \nu\frac{\lambda_{po}}{\lambda_q}, \\ I_1 &= \frac{P_{qf}}{4}\frac{\lambda_b}{\lambda_q - \lambda_p} - \nu\frac{\lambda_{opc}/4}{\lambda_p - \lambda_o} - \nu\frac{\lambda_{opc}/4}{\lambda_q - \lambda_p}, \\ I_2 &= 1 - P_{qf} - \nu\frac{\lambda_{ox}}{\lambda_+ - \lambda_o} - \nu\frac{\lambda_{ox}}{\lambda_q - \lambda_+}, \\ I_3 &= \nu\frac{\lambda_p \lambda_{opc}/4}{\lambda_o(\lambda_p - \lambda_o)} + \nu\frac{\lambda_+ \lambda_{ox}}{\lambda_o(\lambda_+ - \lambda_o)} + \nu\frac{\lambda_{po}}{\lambda_o}. \end{aligned} \tag{10}$$

Particularly when there are no reactions between Ps and oxygen ($\lambda_{opc} = \lambda_{ox} = 0$), these expressions are reduced to:

$$\begin{aligned} I_0 &= P_{qf}\frac{\lambda_{qf}}{\lambda_q} - \frac{P_{qf}}{4}\frac{\lambda_p \lambda_b}{\lambda_q(\lambda_q - \lambda_p)} - \frac{3P_{qf}}{4}\frac{\lambda_{po}\lambda_b}{\lambda_q(\lambda_q - \lambda_{po})}, \\ I_1 &= \frac{P_{qf}}{4}\frac{\lambda_b}{\lambda_q - \lambda_p}, \quad I_2 = 1 - P_{qf}, \quad I_3 = \frac{3P_{qf}}{4}\frac{\lambda_b}{\lambda_q - \lambda_{po}}. \end{aligned} \tag{11}$$

It is easy to verify that in this case $P_{qf} = I_0 + I_1 + I_3$ and $\sum_{i=0}^{3} I_i = 1$. In the case of very fast formation of the Ps bubble ($\lambda_b \to \infty$, $\lambda_q \to \infty$), eqn (11) gives $I_0 = 0$, $I_1 = P_{qf}/4$, $I_2 = 1 - P_{qf}$, $I_3 = 3P_{qf}/4$.

Usually in positron lifetime experiments the short-lived components I_0 and I_1 cannot be resolved using conventional exponential deconvolution, so these intensities are combined in one short-lived component, which is incorrectly identified as the probability of *p*-Ps formation. As a result, a wrong conclusion is made about violation of the "one-to-three" ratio of *p*-Ps and *o*-Ps formation probabilities:

$$\frac{I_0 + I_1}{I_3} = \frac{1}{3} + \frac{4(\lambda_{qf} - \lambda_{po})}{3\lambda_b}. \tag{12}$$

Substituting here the probable values of the rates $\lambda_{qf} \simeq 2$, $\lambda_{po} \simeq 0.5$ and $\lambda_b \simeq 10\text{–}15\ \text{ns}^{-1}$, this ratio increases from 1/3 to $\simeq 1/2$ in accordance with the experimental observations in Fig. 1. Thus, an increase in this ratio is a consequence of the formation and presence of qf-Ps over several dozens of picoseconds, before its transformation into a bubble state.

In essence, the proposed model contains only 5 adjustable parameters: P_{Ps}, $\lambda_{qf} \approx \lambda_+$, λ_{po}, k_{opc}, and k_{ox}, since we fixed λ_b to $20\ \text{ns}^{-1}$ based on AMOC experiments.[16,17]

The conventional approach for processing the LT spectra in liquids consists of their deconvolution into three exponentials decreasing with time. This can be derived from eqn (10), if we neglect the existence of qf-Ps (assuming that the rate constant of the Ps bubble formation λ_b is very large). In this case eqn (1)–(4):

$$\dot{n}_p(t) = \frac{\lambda_{opc}}{4} n_o - \lambda_p n_p, \quad \lambda_p = \lambda_{2\gamma} + \lambda_{po}, \quad n_p(0) = \frac{P_{Ps}}{4}, \tag{13}$$

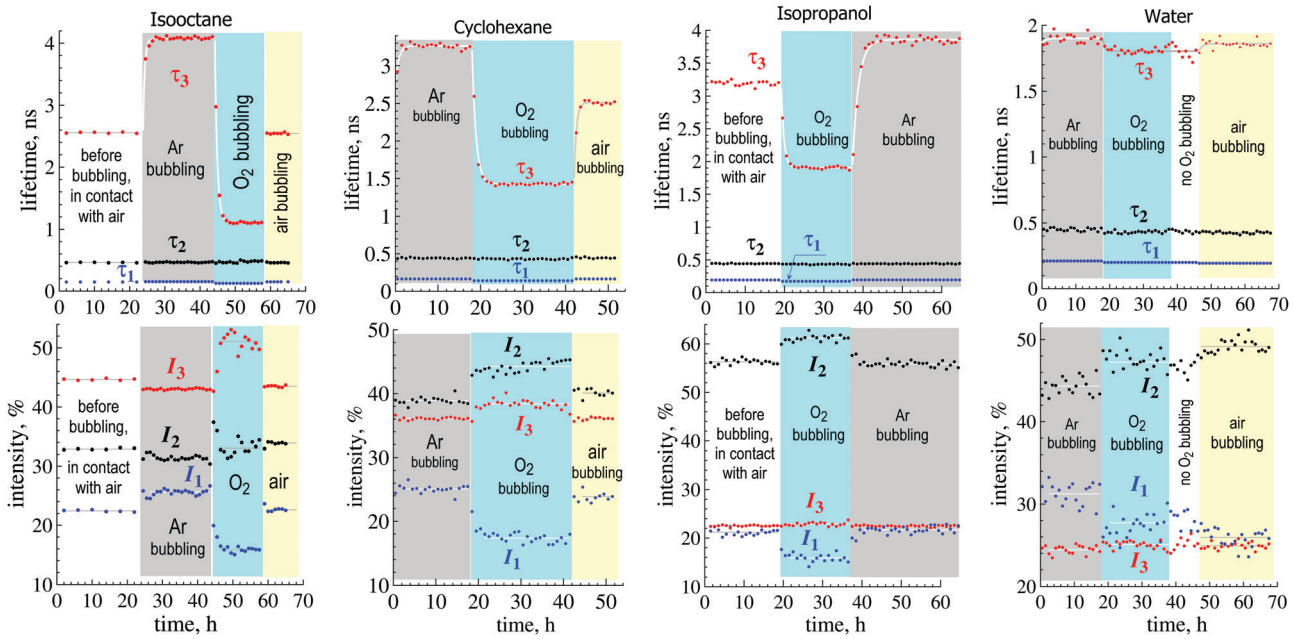

Fig. 1 The parameters of 3-exponential deconvolution of the LT spectra in isooctane, cyclohexane, isopropanol and water before and during bubbling with argon, oxygen and air at room temperature. The lifetime of the shortest (τ_1) component was a "common free" parameter for each stage of the gas bubbling.

$$\dot{n}_+(t) = \lambda_{ox} n_o - \lambda_+ n_+, \quad n_+(0) = 1 - P_{Ps}, \tag{14}$$

$$n_o(t) = \frac{3P_{Ps}}{4} e^{-\lambda_o t}, \quad \lambda_o = \lambda_{po} + \frac{\lambda_{opc}}{4} + \lambda_{ox}. \tag{15}$$

Here P_{Ps} is already the probability of Ps formation just in a bubble state. The equations for n_+ and n_p can easily be solved:

$$n_p(t) = \frac{P_{Ps}}{4} e^{-\lambda_p t} + \frac{3P_{Ps}}{4} \cdot \frac{\lambda_{opc}/4}{\lambda_p - \lambda_o} \left(e^{-\lambda_o t} - e^{-\lambda_p t}\right).$$

$$n_+(t) = (1 - P_{Ps}) e^{-\lambda_+ t} + \frac{3P_{Ps}}{4} \cdot \frac{\lambda_{ox}}{\lambda_+ - \lambda_o} \left(e^{-\lambda_o t} - e^{-\lambda_+ t}\right),$$

after which it turns out that the LT spectrum consists of three exponents:

$$C_{2\gamma}(t) \propto \lambda_+ n_+ + \lambda_p n_p + \lambda_{po} n_o = \lambda_p I_1 e^{-\lambda_p t} + \lambda_+ I_2 e^{-\lambda_+ t} + \lambda_o I_3 e^{-\lambda_o t}, \tag{16}$$

$$I_1 = \frac{P_{Ps}}{4} - \frac{3P_{Ps}}{4} \cdot \frac{\lambda_{opc}/4}{\lambda_p - \lambda_o}, \quad I_2 = 1 - P_{Ps} - \frac{3P_{Ps}}{4} \frac{\lambda_{ox}}{\lambda_+ - \lambda_o}, \tag{17}$$

$$I_3 = \frac{3P_{Ps}}{4} \left[\frac{\lambda_{po}}{\lambda_o} + \frac{\lambda_+}{\lambda_o} \frac{\lambda_{ox}}{\lambda_+ - \lambda_o} + \frac{\lambda_p}{\lambda_o} \frac{\lambda_{opc}/4}{\lambda_p - \lambda_o}\right],$$

$$I_1 + I_2 + I_3 = 1, \quad \tau_1 = \frac{1}{\lambda_p}, \quad \tau_2 = \frac{1}{\lambda_+}, \quad \tau_3 = \frac{1}{\lambda_o}. \tag{18}$$

Such a simplified model (without qf-Ps) cannot explain the observed values of the ratio I_1/I_3 (larger then 1/3). It is seen from eqn (17) and (18) that taking account of the Ps reactions with oxygen (conversion and oxidation; non-zero λ_{ox} and λ_{opc}) reduces the I_1/I_3 ratio even more and brings this model into conflict with experimental data. Therefore, for a formal description of the LT spectra, these quantities I_1, I_2, I_3, τ_1, τ_2 and τ_3 are often considered as free adjustable parameters.

In Fig. 1 and Table 1 we show the results of such a formal treatment of the LT spectra measured in isooctane, cyclohexane, isopropanol and water before and after bubbling argon, oxygen and air through these liquids. The *p*-Ps lifetime τ_1 was assumed to be a "common free" parameter for each stage of gas bubbling. A comparison with the fit when τ_1 was fixed to 125 ps (*p*-Ps lifetime in vacuum) is given in the ESI.‡ The obtained e^+ and *o*-Ps lifetimes are in agreement with the results of previous measurements[8,9] done with deaerated liquids.

4. Concentrations of dissolved O_2 in the studied liquids

Gas solubility is often expressed by the Ostwald coefficient, L, which is the ratio of the gas concentration in the gas phase to its concentration in the liquid: $L = c_{O_2}^{(L)} \Big/ c_{O_2}^{(G)}$ (in some papers, the Ostwald coefficient is defined as $c_{O_2}^{(G)} \Big/ c_{O_2}^{(L)}$).§

When pure oxygen is bubbled through a liquid, its partial pressure is 1 atm and its gas phase concentration is $c_{O_2}^{(G)} \approx 1/24.1$ mole per liter, since at 20 °C 1 mole of an ideal gas occupies 24.1 liters. The concentrations of O_2 in liquids can be easily obtained, knowing the values of the Ostwald coefficients (Table 2): $L = c_{O_2}^{(L)} \Big/ c_{O_2}^{(G)}$. When air is blown through a liquid, the

§ Gas solubility may also be expressed in terms of the mole fraction, x, which is the ratio of the number of moles of the solute (gas molecules) to the total number of moles of all substances per unit volume of the solution.

Table 1 Parameters of the 3-exponential decomposition of the LT spectra of the initially aerated isooctane, cyclohexane, isopropanol and water, and also after their bubbling with argon, oxygen and air at room temperature. τ_1 is considered a "common free" parameter for each gas bubbling. Statistical uncertainties of the fitting parameters are indicated in parentheses

Liquid	I_1, %	τ_1, ps	I_2, %	τ_2, ns	I_3, %	τ_3, ns	$\lambda_o = 1/\tau_3$, ns^{-1}
Isooctane							
– Ar bubbling	24.6	148(1)	32.3(1)	0.45(1)	43.1(1)	4.01(1)	0.249(3)
– Air bubbling	21.8	145(1)	34.4(2)	0.45(1)	43.8(1)	2.51(1)	0.398(5)
– Before bubbling	22.6	149(1)	32.7(1)	0.46(1)	44.7(1)	2.546(3)	0.393(2)
– O_2 bubbling	14	116(3)	31(1)	0.43(1)	55(2)	1.077(6)	0.929(6)
Cyclohexane							
– Ar bubbling	25	165(2)	38.9(4)	0.44(1)	36.1(4)	3.26(4)	0.307(12)
– Air bubbling	23.9	165(2)	40.1(4)	0.45(1)	36.1(4)	2.515(40)	0.398(16)
– O_2 bubbling	17.4	141(2)	44.3(4)	0.43(1)	38.4(4)	1.42(4)	0.703(29)
Isopropanol							
– Ar bubbling	21.7	194(3)	56(1)	0.44(2)	22.5(1)	3.75(10)	0.267(26)
– Before bubbling	21	193(3)	56(1)	0.44(2)	22.5(10)	3.2(1)	0.313(30)
– O_2 bubbling	16	173(4)	61(1)	0.43(2)	22.9(8)	1.905(10)	0.525(6)
Water							
– Ar bubbling	31	213(4)	44(4)	0.44(2)	25(4)	1.833(16)	0.546(9)
– Air bubbling	25	194(3)	49(1)	0.42(2)	25.5(1)	1.802(15)	0.555(9)
– O_2 bubbling	27	200(3)	47(4)	0.42(1)	26(3)	1.746(14)	0.573(8)

Table 2 Values of the Ostwald coefficients $c_{O_2}^{(L)}/c_{O_2}^{(G)}$, concentrations of O_2 in liquids after their bubbling with oxygen and air at room temperature (20 °C) and 1 atm pressure. Values of k_{Ps+O_2} and λ_{po} were obtained by fitting the data shown in Fig. 2, using eqn (19)

Liquid	$c_{O_2}^{(L)}/c_{O_2}^{(G)}$	$c_{O_2}^{(L)}$, M O_2 bubbling $c_{O_2}^{(G)} = 0.4515$ M	$c_{O_2}^{(L)}$, M air bubbling $c_{O_2}^{(G)} = 0.4515$ M	k_{Ps+O_2}, M^{-1} s^{-1}	λ_{po}, ns^{-1}
Isooctane	0.362[18]	0.0148	3.2×10^{-3}	$4.50(6) \times 10^{10}$	0.25(1)
	0.3725[19]	0.0154			
Cyclohexane	0.27[18,20]	0.0112	2.35×10^{-3}	$3.51(7) \times 10^{10}$	0.31(1)
Isopropanol	0.2463[19]	0.010	2.1×10^{-3}	$2.61(6) \times 10^{10}$	0.26(1)
Water	0.0334[18]	0.00139	2.9×10^{-4}	$1.86(10) \times 10^{10}$	0.55(2)

O_2 concentration in the gas phase is 0.21 times less: $c_{O_2}^{(G)} \approx 0.0087$ mole per liter (since partial O_2 pressure in air is 0.21 atm). The O_2 concentration in the liquid phase decreases by the same proportion.

In our experiments dissolved oxygen is completely removed from the liquid phase after 2 hours of bubbling argon through the liquid.

5. Determination of the Ps–O_2 reaction rate constants

If we neglect any influence of the intratrack radiolytic products on Ps (which can also promote Ps oxidation and conversion, although mostly on a short time-scale) and in the absence of dissolved oxygen, the *o*-Ps lifetime is determined only by the pick-off annihilation of e^+ with one of the electrons of nearby molecules. In the presence of O_2, the *o*-Ps lifetime can also be shortened because of conversion to the *para*-state and Ps oxidation:

$$\lambda_o\left(c_{O_2}^{(L)}\right) = \lambda_{po} + \frac{\lambda_{opc}}{4} + \lambda_{ox} = \lambda_{po} + k_{Ps+O_2} \cdot c_{O_2}^{(L)},$$
$$k_{Ps+O_2} = \frac{k_{opc}}{4} + k_{ox}. \quad (19)$$

Our experimental data for $\lambda_o\left(c_{O_2}^{(L)}\right)$ at different O_2 concentrations in liquids are summarized in Tables 1 and 2. Approximating these dependencies using eqn (19), one can determine the values of the "total" rate constant k_{Ps+O_2} reaction with oxygen and the pick-off annihilation rate λ_{po} (see Table 2 and Fig. 2).

In Fig. 3 our data for k_{Ps+O_2} are plotted *vs.* the inverse dynamic viscosity $1/\eta$ of the liquids, together with the previous data for other liquids.[7] The linear dependence of k_{Ps+O_2} over T/η indicates that the Ps + O_2 reaction is diffusion-controlled:

$$k_{Ps+O_2} = 4\pi(D_{Ps} + D_{O_2})(R_{Ps} + R_{O_2}),$$
$$D_{Ps} + D_{O_2} = \frac{k_B T}{4\pi\eta R_{Ps}} + \frac{k_B T}{6\pi\eta R_{O_2}} \propto \frac{T}{\eta}. \quad (20)$$

Here k_B is the Boltzmann constant, T is the absolute temperature, D_{Ps} and D_{O_2} are the diffusion coefficients of the reactants, $R_{Ps} \approx$ 3–4 Å and $R_{O_2} \approx 2$ Å are the bubble radii of Ps and O_2.

Eqn (20) brings us two problems. The first one is that the rate constant should tend to zero with increasing viscosity of the solvent, whereas Fig. 3 shows that it does not (k_{Ps+O_2} remains finite at high viscosity). This means that the interaction of Ps and O_2 occurs not only at a distance of a direct contact with the reactants, but also at greater distances

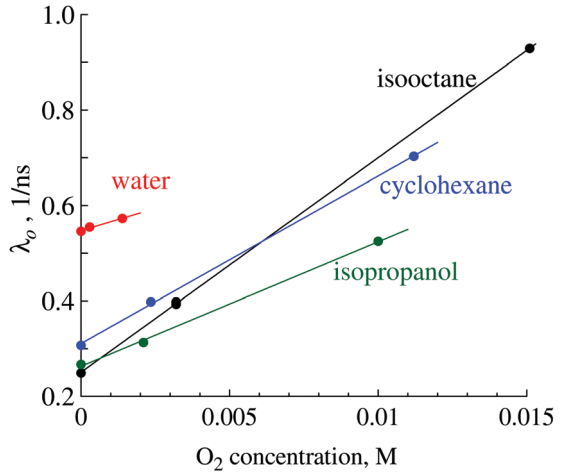

Fig. 2 Dependencies of λ_o (data taken from Table 1) *vs.* concentration of dissolved oxygen in different liquids. Solid lines – eqn (19).

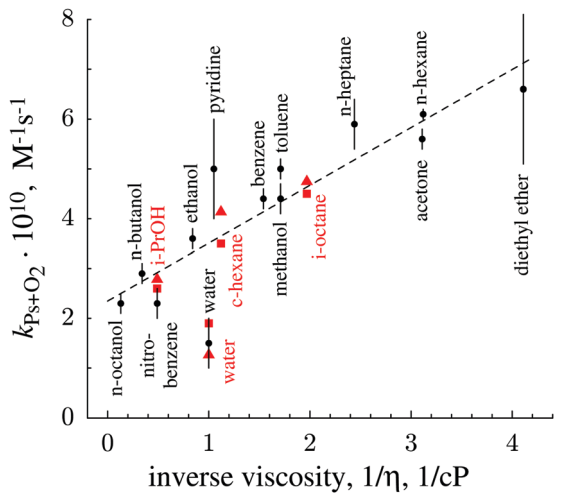

Fig. 3 The linear dependence of the rate constants k_{Ps+O_2} of the Ps reaction with dissolved oxygen in different liquids *vs.* the inverse viscosity, $1/\eta$ eqn (20). Black circles ● are taken from ref. 7; red symbols ▲ and ■ from Tables 2 and 3. All the data correspond to room temperature.

(for example, an electron or Ps as a whole may tunnel to the oxygen molecule).[21] The second problem is that the predicted value of the slope of the dependence k_{Ps+O_2} *versus* $1/\eta$ according to eqn (20) is several times smaller than it really is in Fig. 3. It may indicate that we must distinguish between the reaction radii of the reagents and their "hydrodynamic" radii entering the diffusion coefficients. Seemingly, the reaction radii are larger then the hydrodynamic ones.

6. Processing of the spectra through a model taking into account the formation of qf-Ps

In the present study, we take into account that Ps atoms are not formed in nanobubbles instantly. It takes a certain time to find a pre-existing place suitable for localization (Section 3). More subtle effects such as the time-dependence of the rate constant k_{Ps+O_2} according to the Smoluchowski theory are not considered in this paper.[23]

In Section 5 we discussed only values of the "total" rate constants k_{Ps+O_2} (but not k_{opc} and k_{ox} separately) because it is hardly possible to distinguish the interaction mechanisms of the Ps with O_2 (conversion or oxidation) on the sole basis of the quenching rate constant $\lambda_o\left(c_{O_2}^{(L)}\right)$. However, the equations developed in Section 3 show that the processes of Ps *ortho–para* conversion and Ps oxidation result in different redistributions of the lifetime components (I_i) of the LT spectra. This makes it possible to determine the dominant mechanism of the Ps + O_2 interaction.

In the mid-1960s the Ps + O_2 interaction was generally accepted to be just conversion.[7] However, after the ACAR experiments in deaerated and oxygenated *n*-hexane,[24] this viewpoint was rejected. No increase of the "narrow" parapositronium component in O_2-saturated *n*-hexane was observed. This result points to Ps oxidation by O_2 as the dominant process. However, questions remain about this experiment,[24] as the *o*-Ps lifetime found in oxygen-saturated *n*-hexane (1 ns) was almost two times less than that obtained by other authors.[7–9]

Unfortunately existing software products like LT-10[25] or PALSfit3[26] (http://palsfit.dk/) do not include fitting models that account for the physical behavior outlined in Section 3. Therefore, in order to shed some light on the interaction mechanisms of Ps and O_2, we developed special computer software named "RooPositron" for processing lifetime annihilation spectra (https://github.com/petrstepanov/roopositron).

The program is written in the C++ language and utilizes the ROOT framework[27] developed by CERN. ROOT is a set of object-oriented classes that provide vast functionality for analyzing scientific data. The RooFit[28] package allows the user to build up custom fitting models based on corresponding parameters and performs simultaneous fits of multiple spectra by minimizing the chi-square.

In RooPositron we implemented functionality that is similar to the existing products on the market, such as simultaneous spectra fitting, the ability to fit spectra with various channel widths, introduced common and fixed fitting parameters, graphical visualization of the fit and residuals (Fig. 4), and plot exports to ASCII files.

Some competitive features of the RooPositron program that make it outstanding with respect to existing solutions include:

- RooPositron's code is open-source and the program is distributed free of charge. Any researcher in the field can contribute and improve the functionality.
- The program supports integration of custom fitting models that correspond to meaningful physical parameters of the environment.
- The fitting models support calculation of indirect parameters as functions of the regular parameters of the model.
- Various types of minimizer functions can be used in order to fit the spectra (MINUIT, FUMILI and some others).

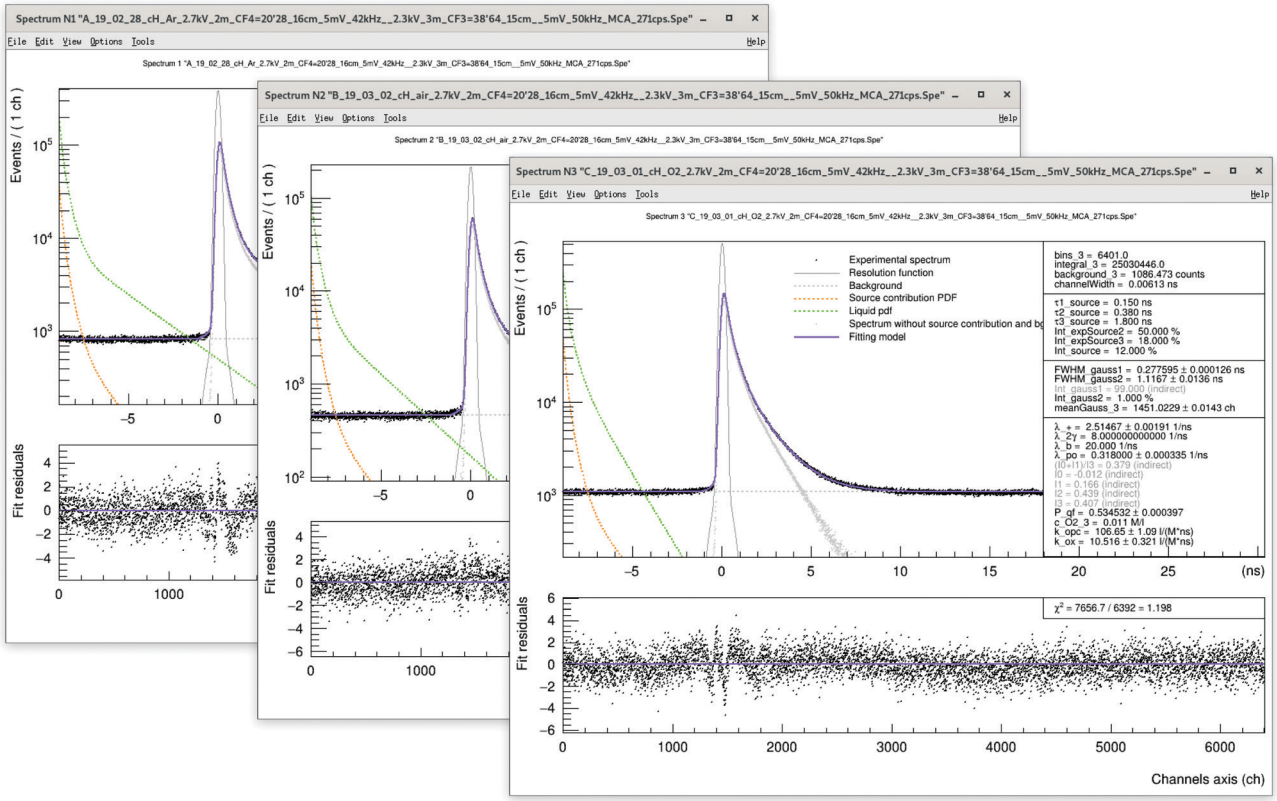

Fig. 4 Screenshots of the RooPositron software[29] depicting a series of spectra fitted with a model derived from eqn (1)–(4).

Table 3 Parameters of the model eqn (5)–(10) obtained as a result of fitting the LT spectra of liquids with different O_2 contents, $\lambda_{qf} = \lambda_+$, $\lambda_b = 20$ ns^{-1}, $\lambda_{2\gamma} = 1/0.16$ ns^{-1} (in accordance with the magnetic quenching experiments[12,13]). Statistical uncertainties of the fitting parameters are indicated in parentheses

Liquid	$\lambda_+ = \lambda_{qf}$, ns^{-1}	$\tau_+ = 1/\lambda_+$, ns	λ_{po}, ns^{-1}	$\tau_{po} = 1/\lambda_{po}$, ns	P_{qf}	k_{opc}, M^{-1} s^{-1}	k_{ox}, M^{-1} s^{-1}	$k_{opc}/4 + k_{ox}$, M^{-1} s^{-1}
Isooctane	2.430(1)	0.412(1)	0.252(1)	3.968(4)	0.639(2)	$9.62(9) \times 10^{10}$	$2.37(3) \times 10$	$4.78(5) \times 10^{10}$
Cyclohexane	2.568(2)	0.389(1)	0.320(3)	3.125(10)	0.542(1)	$12.6(2) \times 10^{10}$	$1.02(4) \times 10^{10}$	$4.17(5) \times 10^{10}$
Isopropanol	2.509(1)	0.399(1)	0.276(2)	3.622(10)	0.340(2)	$9.8(1) \times 10^{10}$	$0.35(5) \times 10^{10}$	$2.82(5) \times 10^{10}$
Water	2.516(8)	0.397(4)	0.556(1)	1.799(2)	0.451(3)	$1(1) \times 10^{10}$	$1.1(4) \times 10^{10}$	$1.3(8) \times 10^{10}$

• The user has control over the convolution operation parameters. By adjusting the convolution binning the user can either select a quicker fitting speed or obtain a higher fit precision.

The program comes with detailed instructions that cover installation and usage and explain how to add custom models. RooPositron is hosted on GitHub (https://github.com/petrstepanov/roopositron).

Currently RooPositron can perform conventional multi-exponential fits, trapping models, and diffusion-trapping models. In this work the program was extended with a fitting model of the formation of a Ps atom in liquid media that accounts for the qf-Ps state, as formulated in Section 3. The integrity of the fitting equations added into the program was additionally verified by the Wolfram Mathematica computing system. Parameters P_{Ps}, $\lambda_{qf} = \lambda_+$, λ_{po}, k_{opc}, and k_{ox} are set as free during the fit. The rate constant of Ps bubble formation λ_b is fixed to 20 ns^{-1} to be in agreement with the AMOC data.[16,17]

All experimental spectra were analyzed and fitted by the proposed model. The obtained parameters, including values of

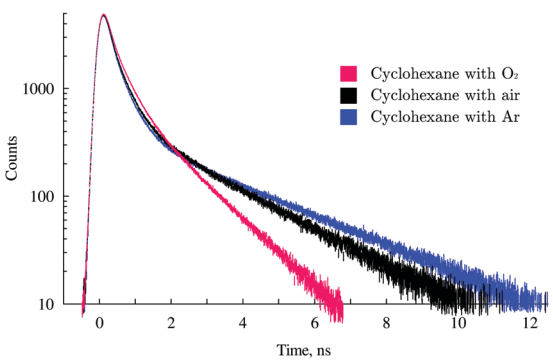

Fig. 5 The effect of the presence of O_2 on the shape of lifetime annihilation spectra in cyclohexane. Blue – blowing with argon, black – blowing with air, red – blowing with oxygen. Source contribution and background are subtracted from the spectra. The spectra are normalized to 10^6 counts.

the Ps spin-conversion rate constant (*ortho*-Ps ⇔ *para*-Ps) and Ps oxidation rate constant ($Ps + O_2 \rightarrow e^+ + O_2^-$), are given in Table 3. Oxidation of the Ps atom turned out to be a 5–10 times less favorable process. In conventional three-exponential deconvolution of the spectra, the Ps–O_2 interaction is manifested in the variation of only one parameter – the *o*-Ps annihilation rate λ_o *vs.* O_2 concentration. It does not allow conversion and oxidation to be distinguished (Fig. 5).

7. Conclusion

The interaction of a Ps atom with oxygen dissolved in liquid media is a rather complex problem. In fact it is a special case of the general problem of random walks of a particle and its acceptors when they can interact over a random distance.[22] The problem is even more complex because the formation of Ps atoms in nanobubbles does not happen at the same moment of time (say, $t = 0$). Instead every formation event happens to have a certain random time delay. These delays occur due to the existence of a delocalized intermediate transient state of an e^+–e^- pair named quasi-free positronium (qf-Ps). The localization event of qf-Ps is preceded by the process of seeking a suitable preexisting trap in the solvent. This aspect is studied in current paper.

Following the spin statistics, it has long been thought that the formation of the *ortho*- and *para*-states of Ps should strictly result in the ratio $I_1/I_3 = 1/3$. However, by taking into account the existence of the qf-Ps as a precursor of the ensuing bubble state of Ps, we were able to explain the anomalously high ratio for I_1/I_3 (1/2 or more) as it is usually found through conventional analysis of the LT spectra into 3 decaying exponential components. Moreover, the proposed model, which takes into account the formation of qf-Ps, naturally explains the extreme behavior of the $S(t)$ parameter (juvenile broadening) observed in AMOC experiments.

The presence of oxygen does not affect the lifetime of ''free'' positrons, $\tau_+ = 1/\lambda_+$. It is mostly determined by the structure of the solvated state e^+ and the average electron density of the solvent.

A new open-source program, RooPositron, that fits lifetime annihilation spectra has been developed.[29] The software supports the integration of custom fitting models. A model derived from eqn (5)–(10) is integrated into the new program as a fitting function. By contrast with the conventional multi-exponential deconvolution, the new fitting model parameters represent values with real physical meaning (such as Ps reaction rate constants, annihilation rate constants of the various positron states, probability of qf-Ps formation, localization rate of qf-Ps in a nanobubble). Application of the RooPositron program revealed the *ortho–para*-conversion of a Ps atom to be a dominant process of the interaction between the Ps atom and dissolved oxygen. Oxidation of the Ps atom turned out to be about 5–10 times less favorable. In conventional three-exponential analysis it is not possible to distinguish between conversion and oxidation.

The spectra of water with dissolved oxygen show almost no difference in shape and fitting parameters with respect to pure water spectra. This is explained by a very low solubility of O_2 molecules. Therefore pure water is often used as a ''reference'' medium for testing the operation of lifetime positron spectrometers.

The experimental part of this research was performed using the facilities of the KAMIKS (http://kamiks.itep.ru/) center of the NRC ''Kurchatov Institute'' – ITEP.

Conflicts of interest

There are no conflicts to declare.

References

1 G. Duplatre and I. Billard, Organic and Inorganic Chemistry of the Positron and Positronium, in *Principles and Applications of Positron & Positronium Chemistry*, ed. Y. C. Jean, P. E. Mallon and D. M. Schrader, World Scientific, Singapore; Hong Kong, 2003.
2 *Positron and Positronium Chemistry*, ed. D. M. Schrader and Y. C. Jean, Studies in physical and theoretical chemistry, Elsevier, Amsterdam [The Netherlands], New York, 1988.
3 G. Consolati, I. Genco, M. Pegoraro and L. Zanderighi, Positron annihilation lifetime (PAL) in poly[1-(trimethylsilyl)propine] (PTMSP): Free volume determination and time dependence of permeability, *J. Polym. Sci., Part B: Polym. Phys.*, 1996, **34**(2), 357–367.
4 B. Jasinska, B. Zgardzinska and G. Cholubek, *et al.*, Human Tissue Investigations Using PALS Technique - Free Radicals Influence, *Acta Phys. Pol., A*, 2017, **132**(5), 1556–1558.
5 E. Kubicz and for the J-PET collaboration, Potential for biomedical applications of positron annihilation lifetime spectroscopy (PALS), *AIP Conf. Proc.*, 2019, **2182**, 050004, DOI: 10.1063/1.5135847.
6 P. Moskal, *et al.*, Feasibility study of the positronium imaging with the J-PET tomograph, *Phys. Med. Biol.*, 2019, **64**, 055017, DOI: 10.1088/1361-6560/aafe20.
7 J. Lee and G. J. Celitans, Oxygen and Nitric Oxide Quenching of Positronium in Liquids, *J. Chem. Phys.*, 1966, **44**, 2506, DOI: 10.1063/1.1727072.
8 Y. Kobayashi, *J. Chem. Soc., Faraday Trans.*, 1991, **87**, 3641.
9 O. E. Mogensen, *Positron Annihilation in Chemistry*, Springer Verlag, Berlin, Heidelberg, New York, London, Paris, Tokyo, Hong Kong, Barcelona, Budapest, 1995.
10 B. Zgardzinska, W. Bialko and B. Jasinska, Ortho-para spin conversion of Ps by paramagnetic O2 dissolved in organic compounds, *Nukleonika*, 2015, **60**(4), 801–804, DOI: 10.1515/nuka-2015-0144.
11 A. Karbowski, K. Fedus, K. Suzewski, J. Bruzdowska and G. Karwasz, *Acta Phys. Pol., A*, 2017, **132**(5), 1466, DOI: 10.12693/APhysPolA.132.1466.
12 A. Bisi, G. Consolati, G. Gambarini and L. Zappa Nuovo Cimento, V.65B(2), p.442 (1981); Nuovo Cimento, V.1D(6), p.725 (1982); Nuovo Cimento, V.5D, p.358 (1985).

13 I. Billard, J.-Ch Abbe and G. Duplatre, *J. Phys. Chem.*, 1991, **95**, 2501.
14 S. V. Stepanov, G. Duplatre, V. M. Byakov, D. S. Zvezhinskiy and V. S. Subrahmanyam, Formation of quasi-free and bubble positronium states in water and aqueous solutions, *Acta Phys. Pol., A*, 2014, **125**(3), 770–774, DOI: 10.12693/APhysPolA.125.770.
15 S. V. Stepanov, V. M. Byakov, G. Duplatre, D. S. Zvezhinskiy, P. S. Stepanov and A. G. Zaluzhnyi, Early processes in positron and positronium chemistry: possible scavenging of epithermal e+ by nitrate ion in aqueous solutions, *J. Phys.: Conf. Ser.*, 2015, **618**, 012003, DOI: 10.1088/1742-6596/618/1/012003.
16 D. S. Zvezhinskiy, M. Butterling, A. Wagner, R. Krause-Rehberg and S. V. Stepanov, Account of the intratrack radiolytic processes for interpretation of the AMOC spectrum of liquid water, *J. Phys.: Conf. Ser.*, 2013, **443**, 012057, DOI: 10.1088/1742-6596/443/1/012057.
17 D. S. Zvezhinskiy, M. Butterling, A. Wagner, R. Krause-Rehberg and S. V. Stepanov, The evidence of quasi-free positronium state in GiPS-AMOC spectra of glycerol, *Acta Phys. Pol., A*, 2014, **125**(3), 821–824, DOI: 10.12693/APhysPolA.125.821.
18 H. L. Clever, R. Battino, H. Miyamoto, Yu. Yampolski and C. L. Young, IUPAC-NIST Solubility Data Series. 103. Oxygen and Ozone in Water, Aqueous Solutions, and Organic Liquids (Supplement to Solubility Data Series Volume 7), *J. Phys. Chem. Ref. Data*, 2014, **43**, 033102, DOI: 10.1063/1.4883876.
19 C. B. Kretschmer, J. Nowakowska and R. Wiebe, Solubility of Oxygen and Nitrogen in Organic Solvents from −25 to 50 °C, *Ind. Eng. Chem.*, 1946, **38**(5), 506–509.
20 R. Battino, T. R. Rettich and T. Tominaga, The Solubility of Oxygen and Ozone inLiquids, *J. Phys. Chem. Ref. Data*, 1983, **12**, 163–178, DOI: 10.1063/1.555680.
21 V. M. Byakov, V. R. Petukhov and J. Radioanal, *Nucl. Chem. Lett.*, 1984, **85**(1), 67.
22 S. V. Stepanov and V. M. Byakov, To the Theory of Nonstationary Diffusion-Controlled Tunnelling Chemical Reactions, *Radiat. Phys. Chem.*, 2003, **68**, 643–646, DOI: 10.1016/S0969-806X(03)00284-6.
23 F. Bockstahl and G. Duplâtre Phys, Quantitative determination of a sodium dodecyl sulfate micellar radius through positron annihilation lifetime spectroscopy, *Phys. Chem. Chem. Phys.*, 1999, **1**, 2767–2772, DOI: 10.1039/A901518C.
24 D. P. Kerr, A. M. Cooper and B. G. Hogg Canad, *J. Phys.*, 1965, **43**, 963.
25 http://prac.us.edu.pl/kansy/index.php?id=lt10.
26 http://palsfit.dk/.
27 I. Antcheva, M. Ballintijn, B. Bellenot, M. Biskup, R. Brun, N. Buncic, Ph. Canal, D. Casadei, O. Couet, V. Fine, L. Franco, G. Ganis, A. Gheata, D. G. Maline, M. Goto, J. Iwaszkiewicz, A. Kreshuk, D. M. Segura, R. Maunder, L. Moneta, A. Naumann, E. Offermann, V. Onuchin, S. Panacek, F. Rademakers, P. Russo and M. Tadel, *Comput. Phys. Commun.*, 2009, **180**, 2499, DOI: 10.1016/j.cpc.2009.08.005.
28 W. Verkerke and D. Kirkby, *RooFit Users Manual v2.91*, http://root.cern.ch/download/doc/RooFit_Users_Manual_2.91-33.pdf.
29 P. Stepanov, *RooPositron, A flexible positron lifetime fitting software*, https://github.com/petrstepanov/roopositron.